EQUILIBRIUM AND KINETICS STUDIES REGARDING THE ADSORPTION OF COPPER(II) IONS BY VARIOUS TYPES OF CHITOSAN BEADS

B. VLAD-OROS[a,b,c], D. DASCALU[a,b], Z. DUDAS[c], H. POPOVICI[a],
G. PREDA[a,b], V. OSTAFE[a,b,*]
[a]*West University of Timisoara, Faculty of Chemistry, Biology, Geography, Department of Biology - Chemistry, 16 Pestalozzi, 300115 Timisoara, Romania,*
[a]*West University of Timisoara, Advanced Environmental Research Laboratory, 4 Oituz, 300086, Timisoara, Romania*
[c]*University „Al. I. Cuza" from Iasi, 11 Carol I, Iasi, Romania (temporally affiliated)*
[d]*Institute of Chemistry Timisoara of Romanian Academy, 24 Mihai Viteazul, 300223 Timisoara, Romania*

Two different types of chitosan (low and medium molecular weight) and two different methods were used to prepare chitosan beads. Their efficiency for the removal of Cu(II) ions from aqueous solution was investigated. In order to characterize the chitosan beads BET surface area analysis, Fourier transform infrared spectroscopy and thermogravimetric techniques were used. All types of chitosan beads presented good adsorption capacities. Langmuir and Freundlich isotherms theories were used to fit the equilibrium adsorption data. Adsorption of Cu(II) ions on all types of chitosan beads followed pseudo-second order kinetics.

1. Introduction

Heavy metals occurrence in the environment in high concentration represents a risk not only for human health but also for other living beings because of their toxicity [1]. Many industrial processes, i.e. mining, electroplating, dyeing, paper and petroleum, pollute the environment, contaminating the soil and the surface water streams with waste water which contains metallic ions, such as Cr^{3+}, Ni^{2+}, Zn^{2+}, Cu^{2+}, Pb^{2+} and Cd^{2+}. Among heavy metal ions, Cu(II) ions were extensive studied, due to their usage in various industries. In very small quantities, copper is an essential element to humans, but in high dosage, it may have a series of negative effects. Short periods of exposure cause gastro-intestinal troubles, nausea and vomit. In years, the use of water with a copper content that exceeds the admitted limit can cause serious liver and/or kidney problems, the Wilson disease, insomnia [2, 3].

Numerous procedures of eliminating copper from wastewater have been proposed: precipitation, ion exchange, adsorption, membrane filtration (ultrafiltration, reverse osmosis, electrodialysis etc.), coagulation-electrocoagulation and flocculation, etc. [2, 4-7]. Among these methods, adsorption proved to be one of the most efficient. In the lasts decades, the quest for the development of new or improved, cheap and easy-to-use adsorbent has been a priority [1]. Due to their abundant availability, low-cost and eco-friendly behaviour, different biopolymers were used as adsorbents in order to remove heavy metals from wastewaters. Among these biopolymers, chitosan, a polycationic polymer (Figure 1) and waste product from the sea-food processing

---

*Corresponding author: vostafe@cbg.uvt.ro

industry, is of great intrest [8]. Chitosan has, among other properties (non-toxic, biodegradable, anti-bacterial, etc.), a very functional one, namely to bind selectively different materials i.e. metal ions, fats, cholesterols, proteins, etc. [8, 9]. Due to its large number of amino ($-NH_2$) and hydroxyl ($-OH$) groups that function as coordination and reaction sites, high hidrophilicity and flexible structure of its chain, chitosan is a good natural adsorbent for metal ions [7, 10].
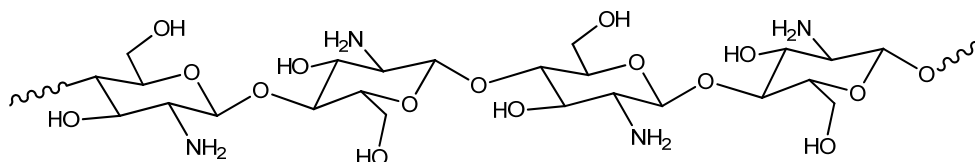

Fig. 1 Chemical structure of chitosan

Chitosan gel beads, used for the uptake of metal ions in the adsorption process, can be prepared through different methods. The polymer disolved in acetic acid is extruded into an alkaline coagulation bath or an ionotropic gelation media, consisting of tripolyphosphate ions [11]. Tripolyphosphate (TPP), a polyanion, will interact with the protonated amine groups of chitosan through electrostatic forces (Fig. 2) [12].
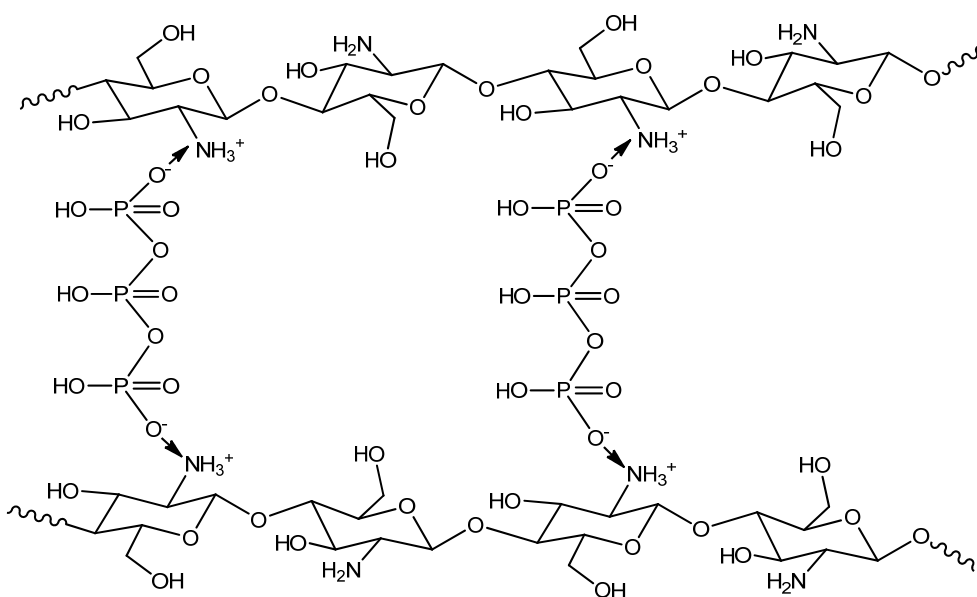

Fig. 2 Chitosan-tripolyphosphate network

The physicochemical properties of chitosan depend considerably on its degree of deacetylation, molecular weight and crystallinity [11]. Previous studies showed that chitosan presents low porosity and weak mechanical properties so future research must be performed in order to overcome its disadvantages, to improve its adsorption capacity and to produce optimal materials for various applications [6].

The aim of the present paper is to study the influence of the chitosan molecular weight and of the preparation method of chitosan beads on the adsorption process. Thus, by using low and medium molecular weight chitosan and two methods of synthesis, different types of chitosan beads were prepared and used for the removal of Cu(II) ions from synthetic solutions. The beads were characterized using BET, Fourier transform infrared spectroscopy (FT-IR) and thermogravimetric techniques. The equilibrium adsorption data were evaluated with the use of Langmuir and Freundlich isotherms. The kinetics constants were determined based on the pseudo-first and second order kinetic and Weber-Morris - intraparticle diffusion models.

2. Materials and methods

2.1 Materials

Chitosan (CHS) with low molecular weight (LMW) and medium molecular weight (MMW), with 75-85% degree of deacetylation, were purchased from Fluka (product number 448869 and 448877, respectively). Sodium tripolyphosphate (TPP) (product number 238503), NaOH (product number 30620) and $CuSO_4·5H_2O$ (product number 209198) were procured from Sigma-Aldrich. All the reagents used were of analytical grade.

2.2 Preparation of chitosan beads

Chitosan solutions were prepared by dissolving 2 g of chitosan (LMW and MMW respectively) in 60 mL of 5% acetic acid and left over night. Then, each chitosan solution was extruded dropwise, through a syringe needle, into 500 mL of 0.5 M NaOH solution (pH 14) or 500 mL 3% tripolyphosphate (TPP) solution (pH 8), respectively, under continuous stirring. The beads were filtered and washed several times with distilled water till neutral pH.

2.3 Characterization of chitosan beads

The N_2 sorption isotherm was obtained using a Quantachrome Nova 1200e surface area and pore size analyser (Quantachrome Instruments, Boynton Beach, USA). The surface area was determined with BET and Langmuir method, the pore diameter with BJH and the total pore volume calculated from the maximum gas adsorption volume.

The samples were characterized by Fourier transform infrared spectroscopy (FT-IR), using the KBr pellet method. The IR spectra were recorded using a Jasco 430 FT-IR analyser (Jasco Analytical Instruments, Easton, USA). The spectra were collected at the resolution of 4 cm^{-1} and 32 scans of the region from 4000 to 400 cm^{-1}.

Thermogravimetric analyses were performed with a TGA/SDTA 851-LF Mettler-Toledo apparatus (Mettler-Toledo, Greifensee, Switzerland), in air atmosphere, in the 25°C to 800°C temperature range, with a heating rate of 10 C·min^{-1}.

Percentage of water contained by the chitosan beads was calculated with the equation

$$W\% = \frac{W_w - W_d}{W_w} \cdot 100 \tag{1}$$

where W% is the water regain factor, W_w and W_d are weights (g) of the wet and dried samples, respectively [13].

2.4 Copper(II) ions adsorption experiments

The experiments were carried out using 1 g of adsorbent in 50 mL Cu(II) solutions of 25 mg/L concentration. The effect of contact time, the adsorption equilibrium and the kinetics studies were conducted at room temperature, at pH 5 and under a stirring rate of 100 rpm.

The concentration of Cu(II) ions was analysed at 325 nm using an atomic absorption spectrophotometer (SpectrAA 20 Plus Varian).

The adsorption capacity, q_e (mg/g) was calculated using the following equation:

$$q_e = \left(\frac{C_0 - C_e}{w}\right) V \tag{2}$$

where C_0 is the initial concentration of Cu(II) ions (mg/L), C_e is the equilibrium concentration of Cu(II) ions (mg/L), V is the volume of Cu(II) ions solution (mL) and w is the weight of the chitosan beads (g) used.

3. Results and discussions

3.1 Characterization of chitosan beads

Chitosan beads were prepared from LMW and MMW chitosan solutions extruded in NaOH or TPP solutions. Four types of chitosan beads were obtained: CHSLMW, CHSLMWTPP, CHSMMW and CHSMMWTPP, respectively. The samples were characterized by surface measurements, FT-IR spectroscopy and thermogravimetric analysis.

For the textural characterization of the chitosan beads the N_2 sorption isotherm was recorded. All the analysed samples gave the same IVth type isotherm with H3 hysteresis [14], characteristic for mesoporous materials with slit shaped porosity. The textural characteristics determined from the isotherms are presented in Table 1.

Table 1: Physical properties of different chitosan beads

Type of chitosan beads	W%	BET surface area (S_{BET}, m^2/g)	Langmuir surface area (m^2/g)	Pore volume (V_p, cm^3/g)	Average pore diameter (D_p, nm)
CHSLMW	96.75	0.10	0.18	$2.67 \cdot 10^{-3}$	1.99
CHSLMWTPP	92.31	1.84	3.05	$3.16 \cdot 10^{-3}$	3.61
CHSMMW	96.01	0.99	1.43	$2.56 \cdot 10^{-3}$	2.35
CHSMMWTPP	89.15	0.71	1.43	$5.13 \cdot 10^{-4}$	4.76

For all the samples very low surface was determined, but the obtained results are in accordance with the literature [12, 15]. Lower pore dimension was obtained for the samples synthesized with NaOH than for those with TPP. Also there is an influence of the molecular weight of the chitosan, i.e. by using chitosan with higher molecular weight beads with larger diameter of the pores were obtained. Water regain factor was lower in the case of both CHSTPP samples, indicating that these beads are denser.

In order to confirm the existence of functional groups in the chitosan beads, the FT-IR spectra of the four products were recorded (Figure 3).
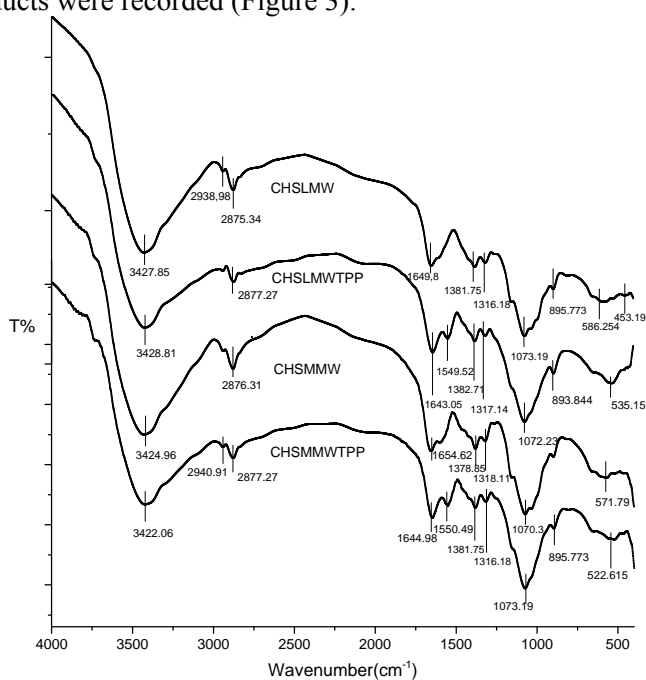

Fig. 3 FTIR spectra of different types of chitosan beads

The FT-IR spectrum of chitosan is complex due to the network of hydrogen bonds which involves –OH, CO and –NH₂ groups [16]. For all types of chitosan beads, the peaks positioned around 3420 cm^{-1} correspond to the stretching vibration of –OH and –NH₂ groups. The bands around 2940 cm^{-1} and 2875 cm^{-1} represent the asymmetrical and symmetrical stretching frequencies of C–H bond in CH₂ and CH groups, respectively [17]. The peaks around 1650 cm^{-1} may be assigned to the deformation of the N–H bond of amino group or to the secondary amide C=O bond of the remaining acetamido groups (amide I band) [18]. The bands around 1380 cm^{-1} are due to the C–H symmetric bending in CHOH. The C–N stretching vibration is represented by the peaks around 1320 cm^{-1}. The large bands at about 1070 cm^{-1} correspond to the C–O stretching vibration in C–OH and C–O–C. In the case of CHSTPP spectra, the peak around 1650 cm^{-1} correspond to PO of the P–OH groups of the tripolyphosphate molecule. The bands around 1550 cm^{-1} are due to $-NH_3^+$ bending in chitosan-tripolyphosphate beads [12]. These bands not present in the NaOH treated chitosan, indicate the involvement of NH₂ groups in the gelation process in the presence of TPP. The spectra suggest that the structural integrity of chitosan is preserved in the beads, being quite similar regardless the molecular weight or the extrusion medium.

The thermograms indicate four weight-loss steps. In the first step (25-200°C), the physically and weak hydrogen bonded water are eliminated. The water elimination is accompanied by an endothermic effect on the DTA curve (Figure 4) [19]. The weight losses in this domain were between 8.52% and 10.31% (Table 2).
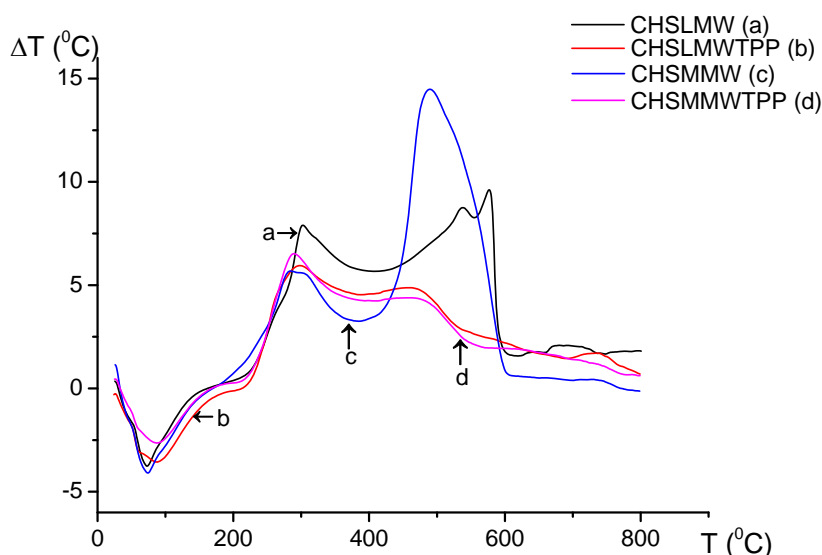

Fig. 4 Thermogravimetric curve of chitosan beads

Table 2: The thermal behaviour and weight losses of obtained chitosan samples

Types of chitosan beads	1st stage (25-200°C)		2nd stage (200-370°C)		3rd Stage (370-600°C)		4th stage (600-800°C)		Total weight loss (%)
	T (°C)	Weight loss (%)	T (°C)	Weight loss (%)	T (°C)	Weight loss (%)	T (°C)	Weight loss (%)	
CHLMW	73	8.52	303	52.26	537 576	98.38	-	0	99.29
CHLMWTPP	90	10.31	298	43.16	460	34.87	737	43.22	81.15
CHSMMW	74	9.41	285	50.21	490	93.53	-	17.61	97.6
CHSMMWTPP	87	9.43	290	45.06	459	38.85	-	38.97	81.43

In stage two, the weight loss is caused by the depolymerisation of chitosan chains, decomposition of pyranose rings through dehydration and deamination and finally ring-opening

reaction [20]. In stage three, the main weight loss corresponds to the degradation of residual cross-liked chitosan. For the samples obtained with NaOH, the predominant stage of thermal degradation appears at stage two (200-370°C) and three (370-600°C). The samples obtained with TPP suffer the predominant degradation in stage two. The additional weight loss, observed beyond 600°C, can be assigned to the decomposition of structural hydroxyl group and partially to the loss of organic residue. The TPP treated chitosan samples presented a better thermal stability (about 81% total weight loss) comparative to the NaOH treated chitosan (98-99% total weight loss). Furthermore, comparing the DTA curves of the low (a) and medium molecular weight (b) samples, it could be observed that both CHSTPP samples had nearly identical thermogram, irrespective of the chitosan molecular weight. The CHSLMW loss all the weight until the final of the third stage, but the CHSMMW suffered a low molecular loss on the fourth stage.

3.2 The effect of contact time on adsorption of Cu(II) ions on chitosan beads

The adsorption capacity of the chitosan beads depending on the contact time between the solution and the adsorbent was studied and the results are presented in Figure 5.
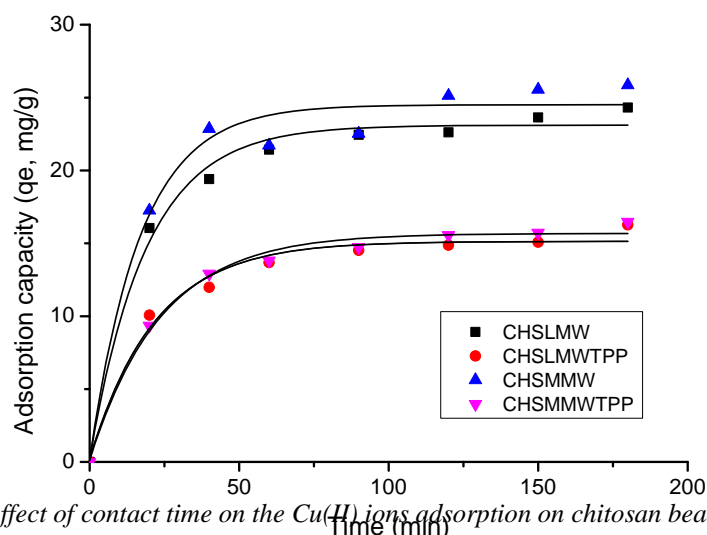

Fig. 5 The effect of contact time on the Cu(II) ions adsorption on chitosan beads

From Figure 5, it can be observed that in all cases the process of sorption has two phases: the first one is rapid, lasting from few minutes till 40 minutes and the second, slow, continues from 2 hours till 24 hours. The chitosan adsorption capacity increases to a certain value with the increase of the contact time then it remains almost constant. Furthermore, CHSMMW showed the best adsorption capacity. Both type of chitosan-TPP beads presented similar behaviour, with an uptake capacity drastically decreased probably because of less adsorption sites available.

3.3 Equilibrium adsorption isotherms

Two isotherm theories have been used to describe the adsorption system. The Freundlich isotherm model is based on an exponential distribution of sorption sites and energies [3]. The linear form of the Freundlich isotherm is represented by the equation:

$$\log q_e = \log k_f + \frac{1}{n}\log C_e \qquad (3)$$

where q_e is the amount of Cu(II) adsorbed per unit weight of the sorbent (mg/g), C_e is the equilibrium concentration of Cu(II) in solution (mg/L), k_f is a measure of adsorption capacity and n is the adsorption intensity (heterogeneity factor).

Langmuir model presumes that there are no interactions between adsorbed species, the surface of the adsorbent has homogenous binding sites and the sorption energies are equivalent [3]. The Langmuir isotherm model can be represented in the form of equation:

$$\frac{C_e}{q_e} = \frac{1}{Q_0 b} + \frac{C_e}{Q_0} \qquad (4)$$

where Q_0 is the amount of adsorbate at complete monolayer coverage (mg/g), which gives the maximum sorption capacity of the sorbent, and b (L/mg) is the Langmuir isotherm constant that relates to the energy of adsorption [21].

The values obtained for both isotherm constants and the regression coefficients (R^2) are given in Table 3.

Table 3: Langmuir and Freundlich isotherm constants and regression coefficient R^2 for the adsorption of Cu(II) ions onto the chitosan beads.

Adsorbent	Langmuir				Freundlich			
	Q_0 (mg/g)	b (L/mg)	R_L	R^2	k_f (mg/g)	1/n	n	R^2
CHSLMW	12.903	0.404	0.096	0.986	51.880	0.474	2.109	0.964
CHSLMWTPP	8.403	0.393	0.092	0.981	32.584	0.449	2.227	0.946
CHSMMW	13.333	0.311	0.114	0.983	70.469	0.545	1.835	0.967
CHSMMWTPP	7.937	0.393	0.092	0.974	31.842	0.449	2.227	0.927

Based on the values of R^2, all types of chitosan beads had a good fit to both Langmuir and Freundlich models, indicating that monolayer and heterogeneous adsorption process may coexist, but monolayer adsorption is probably more dominant. The adsorption process possibly implicates few mechanisms such as ion-exchange, surface complexation or electrostatic attraction [18]. Furthermore, the constant R_L was used to determine if the adsorption process is favourable or unfavourable for Langmuir model [22]

$$R_L = \frac{1}{1+bC_0} \qquad (5)$$

where b is Langmuir isotherm constant, C_0 initial concentration of Cu(II) in solution (mg/L). The R_L values indicate if the adsorption is favourable ($0 < R_L < 1$), unfavourable ($R_L > 1$), linear ($R_L = 1$) or irreversible ($R_L = 0$). The calculated R_L values were between 0 and 1 showing a favourable adsorption of Cu(II) ions.

The maximum adsorption capacity (Q_0) was obtained in the case of CHSMMW and the lowest one for CHSMMWTPP. The values of the Langmuir constant b, related to the affinity of binding sites, showed that CHSLMW had the highest affinity for Cu(II) ions.

In the case of Freundlich model, all the values obtained for parameter n, which indicate the favourability of the adsorption, are higher than 1 showing that the adsorption intensity is good at high concentrations and less at lower ones. The parameter n represented as 1/n is related to the degree of surface heterogeneity. Smaller 1/n values indicate more heterogeneous surface while values closer to one indicate that the adsorbent has relatively more homogeneous binding sites [12]. The 1/n values obtained were between 0.449 and 0.545 showing that for the adsorption of Cu(II) ions, the binding sites involved were more heterogeneous. The relative adsorption capacity is indicated by the k_f values [10]. The k_f values indicated a similar trend as Q_0, the highest k_f value being obtained also in the case of CHSMMW.

3.4 Kinetics of adsorption

In order to investigate the mechanism of adsorption, kinetic data was analysed using Lagergren (pseudo-first-order), pseudo-second-order kinetic equations and Weber-Morris intraparticle diffusion model. The first-order kinetic model describes the reversible equilibrium between liquid and solid phases. The second-order kinetic process assumes that the rate limiting step could be the chemical sorption [3]. The adsorption of the Cu(II) ions on the chitosan beads can occur in one or more steps that may include film or external diffusion, pore diffusion, surface diffusion and adsorption on the pore surface [10].

In the case of pseudo-first-order kinetics, the rate of the adsorptive interactions can be calculated with the Lagergren equation. Liniarized form of this equation is:

$$\log(q_e - q_t) = \log q_e - \frac{k_1}{2.303}t \qquad (6)$$

where q_e and q_t are the amounts of adsorbed Cu(II) ions (mg/g) at equilibrium and time t, respectively, and k_1 (min^{-1}) is the rate constant of pseudo-first-order adsorption. The q_e and k_1 were determined by plotting the $\log(q_e-q_t)$ versus t (Figure 6) and the values obtained are presented in Table 4.

The pseudo-second-order equation can be written as [23]:

$$\frac{dq_t}{dt} = k_2(q_e - q_t)^2 \qquad (7)$$

where k_2 (g/mg·min) is the rate constant of sorption, q_e is the amount of Cu(II) adsorbed (mg/g) at equilibrium and q_t is the amount of the adsorption (mg/g) at any time t. Linearized form of the above equation is:

$$\frac{t}{q_t} = \frac{1}{k_2 q_e^2} + \frac{t}{q_e} \qquad (8)$$

The pseudo-second-order rate constant, k_2 and q_e were calculated from the slope and intercept of the plots t/q_t versus t (Figure 7) and the results are shown in Table 4.
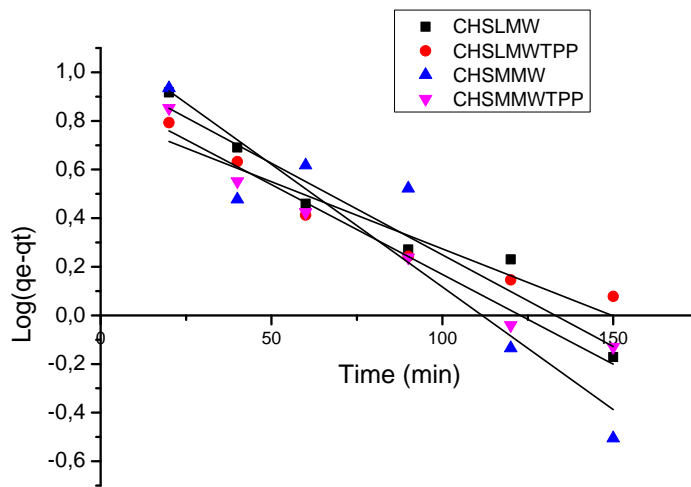

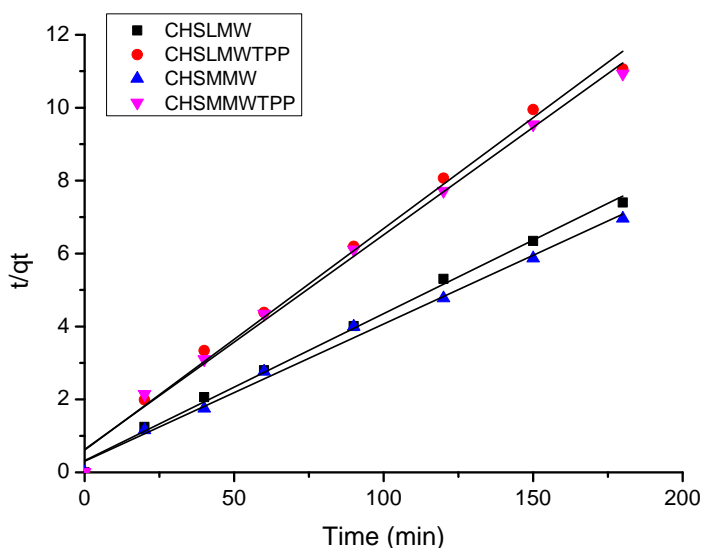*Fig. 6 Pseudo-first order plot of the adsorption of Cu(II) ions on chitosan beads*

Fig. 7 Pseudo-second order plot of the adsorption of Cu(II) ions on chitosan beads

Table 4: Kinetics parameters for the adsorption of Cu(II) ions onto chitosan beads based on pseudo-first and -second order equation

Adsorbent	Pseudo-first order			Pseudo-second order			$q_{e\ experimental}$ (mg/g)
	R^2	q_e (mg/g)	k_1 (min^{-1})	R^2	q_e (mg/g)	k_2 (g/mg·min)	
CHSLMW	0.952	10.051	0.017	0.996	24.814	0.005	24.316
CHSLMWTPP	0.930	6.683	0.012	0.992	16.667	0.006	16.274
CHSMMW	0.874	13.335	0.023	0.993	27.027	0.005	25.862
CHSMMWTPP	0.967	8.054	0.016	0.993	17.241	0.005	16.467

In the case of pseudo-first order kinetics, the data obtained for all chitosan beads have lower R^2 coefficients. In addition, calculated q_e values and experimental q_e values are very different indicating a poor fit to the pseudo-first order kinetic model. The experimental data fit better to the pseudo-second order equation, where the R^2 is higher than 0.99 and the q_e values, both calculated and experimental, are very similar. Thus, chemisorption is the rate limiting step of Cu(II) adsorption on chitosan beads. Probably, during adsorption, valence forces are involved through sharing or exchange of electrons between Cu(II) ions and chitosan binding sites [12, 15]. The Weber-Morris intraparticle diffusion model is described by the equation:

$$Q_t = k_{id}t^{1/2} + C \tag{9}$$

where Q_t (mg/L) is the amount adsorbed at time t (min), and k_{id} (mg/g·min) is the rate constant of intraparticle diffusion. The intercept, C, gives information about the boundary layer thickness, namely the bigger the intercept, the higher is the boundary layer effect [17].

The plots of Q_t vs. $t^{1/2}$ obtained for the adsorption of Cu(II) ions on chitosan beads are shown in Figure 8. The values of intraparticle diffusion rate constant and intercept C are given in Table 5.
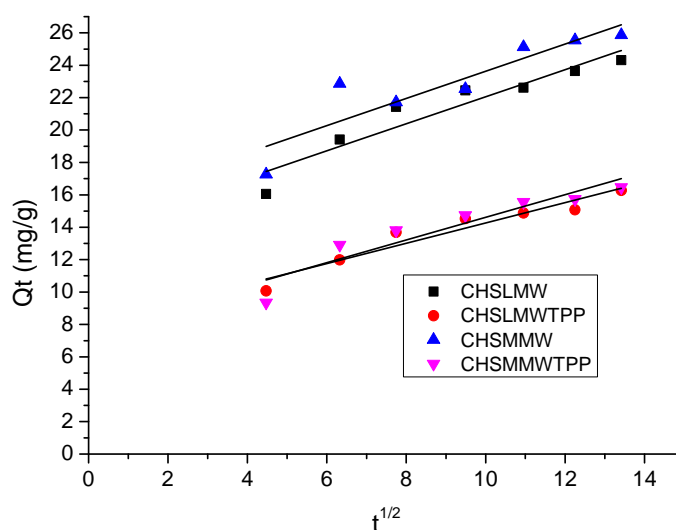
Fig. 8 Weber-Morris intraparticle diffusion kinetics for the adsorption of Cu(II) ions on different types of chitosan beads

Table 5: Kinetics parameters for the adsorption of Cu(II) ions onto chitosan beads based on Weber-Morris - intraparticle diffusion equation

Adsorbent	R^2	k_{id} $(mg/g \cdot min^{1/2})$	C (mg/g)
CHSLMW	0.900	0.834	13.713
CHSLMWTPP	0.927	0.626	7.998
CHSMMW	0.820	0.839	15.230
CHSMMWTPP	0.882	0.699	7.618

The values of regression coefficients (R^2) for the intraparticle diffusion model are lower than that of the pseudo-second order kinetic model so it cannot be considered as the rate controlling step of Cu(II) ions on all types of chitosan beads. In all the cases, the lines did not pass the origin, also showing that intraparticle diffusion is not the rate-controlling step [10].

4. Conclusions

The data show that both types of chitosan, low and medium molecular weight, are good adsorbents for the removal of Cu(II) from aqueous solutions. However CHSMMW presented a better adsorption capacity than CHSLMW. Furthermore, cross-linking with TPP decreased equally the adsorption capacity of both types of chitosan. The surface analysis showed that medium molecular weight chitosan had pores with larger diameter than low molecular weight chitosan while CHSTPP had increased volume and diameter of pores. Thermal stability of the CHSMMW is higher than CHSLMW. The chitosan beads cross-linked with TPP had greater thermal stability, regardless the chitosan molecular weight. The adsorption equilibrium data indicate that Langmuir model provides better fit than Freundlich model, suggesting a monolayer sorption of Cu(II) on all types of chitosan beads. CHSMMW had the highest adsorption capacity (13.33 mg/g). The contact time study showed that the equilibrium is reached after approximately 3 hours. The kinetic experiments indicate that adsorption followed the pseudo-second order kinetic model, so chemisorption is the rate controlling mechanism.

Acknowledgement

References

[1] E. Repo, J. K. Warchol, A. Bhatnagar, M. Sillanpaa, J. Colloid. Interf. Sci. **358**, 261 (2011).
[2] O. Bizerea Spiridon, L. Pitulice, D. Dascalu, B. Vlad-Oros, R. Ionel, V. Ostafe, L. Todorovic, Ann.W.U.T-Ser. Chem. **20**, 45 (2011).
[3] Y. Vijaya, S. R. Popuri, V. M. Boddu, A. Krishnaiah, Carbohyd. Polym. **72**, 261 (2008).
[4] T. A. Kurniawan, G. Y. S. Chan, W. H. Lo, S. Babel, Chem. Eng. J. **118**, 83 (2006).
[5] F. Fu, Q. Wang, J. Environ. Manage. **92**, 407 (2011).
[6] F. Renault, B. Sancey, P. M. Badot, G. Crini, Eur. Polym. J. **45**, 1337 (2009).
[7] A. Bhatnagar, M. Sillanpaa, Adv. Colloid Interfac. **152**, 26 (2009).
[8] Q. Li, E. T. Dunn, E. W. Grandmaison, M. F. A. Goosen, J. Bioact. Compat. Polym. **7**, 370 (1992).
[9] M. Y. Lee, K. J. Hong, T. Kajiuchi, J. W. Yang, Int. J. Biol. Macromol. **36**, 152 (2005).
[10] W. S. W. Ngah, S. Fatinathan, Chem. Eng. J. **143**, 62 (2008).
[11] E. Guibal, Prog. Polym. Sci. **30**, 71 (2005).
[12] W. S. W. Ngah, S. Fatinathan, J. Environ. Manage. **91**, 958 (2010).
[13] X. Li, Y. Li, Z. Ye, Chem. Eng. J. **178**, 60 (2011).
[14] C. G. V. Burgess, D. H. Everett, S. Nuttall, Pure Appl. Chem. **61**, 1845 (1989).
[15] M. L. Dalida, A. F. Mariano, C. M. Futalan, C. C. Kan, W. C. Tsai, M. W. Wan, Desalination **275**, 154 (2011).
[16] J. Zawadzki, H. Kaczmarek, Carbohyd. Polym. **80**, 394 (2010).
[17] S. K. Nadavala, K. Swayampakula, V. M. Boddu, K. Abburi, J. Hazard. Mater. **162**, 482 (2009).
[18] W. S. W. Ngah, S. Fatinathan, J. Environ. Sci. **22**, 338 (2010).
[19] C. G. T. Neto, J. A. Giacometti, A. E. Job, F. C. Ferreira, J. L. C. Fonseca, M. R. Pereira, Carbohyd. Polym. **62**, 97 (2005).
[20] C. Y. Ou, C. H. Zhang, S. D. Li, L. Yang, J. J. Dong, X. L. Mo, M. T. Zeng, Carbohyd. Polym. **82**, 1284 (2010).
[21] S. Meenakshi, N. Viswanathan, J. Colloid. Interf. Sci. **308**, 438 (2007).
[22] Z. Bekci, C. Ozveri, Y. Seki, K. Yurdakoc, J. Hazard. Mater. **154**, 254 (2008).
[23] K. Fujiwara, A. Ramesh, T. Maki, H. Hasegawa, K. Ueda, J. Hazard. Mater. **146**, 39 (2007).